

Energy and force transition between atoms and continuum in quasicontinuum method

Shu-Wei Chang¹, Ying-Pao Liao¹, Chang-Wei Huang² and Chuin-Shan Chen^{*1}

¹Department of Civil Engineering, National Taiwan University, Taiwan

²Department of Civil Engineering, Chung-Yuan Christian University, Taiwan

(Received October 23, 2013, Revised November 1, 2013, Accepted November 11, 2013)

Abstract. We present a full energy and force formulation of the quasicontinuum method with non-local and local transition elements. Non-local transition elements are developed to transmit inhomogeneity from the atomistic to the continuum regions. Local transition elements are developed to resolve the mathematical mismatch between non-local atoms and the local continuum. The rationale behind these transition elements is provided by analyzing the energy and force transitions between atoms and continuum under the Cauchy-Born rule. We show that breakdown of the Cauchy-Born rule occurs for slaved atoms of local elements within the cutoff of non-local atoms. The inadequacy of the Cauchy-Born rule at the transition region naturally leads to the need of atomistic treatment of transition slaved and transition representative atoms. Such an atomistic treatment together with a full or cutoff sampling allows non-local transition elements containing these transition entities to transmit inhomogeneity. Different force formulations for transition representative atoms and pure local representative atoms allow the local transition elements to resolve non-local and local mismatches. The method presented herein is validated by force calculations in an unstressed perfect crystal as well as an unrelaxed grain boundary model. A nanoindentation simulation in 3D is conducted to demonstrate the accuracy and efficiency of the proposed method.

Keywords: quasicontinuum; transition; atomistic model; finite elements

1. Introduction

Atomistic modeling has been used to address a wide variety of deformation processes in solids recently (Chen *et al.* 2008, Chan *et al.* 2011, Lai and Chen 2013, Chen and Lee 2010, Jeong *et al.* 2011, Shen 2013, Teng *et al.* 2011, Wang *et al.* 2013, Zhao and Aluru 2008). The advantage of fully atomistic modeling is its capability to provide desirable resolution that accounts for highly inhomogeneous deformations caused by lattice defects in materials. On the other hand, the weakness of the atomistic approach is that it must incorporate a significant number of redundant degrees of freedom for atoms that are relatively far away from the defects. Thus, the application of fully atomistic modeling is limited by available computing resources. This limitation often prevents researchers from modeling realistic structures for sizes that exceed a few hundred nanometers.

*Corresponding author, Professor, E-mail: dchen@ntu.edu.tw

The resulting length scale restriction represents a substantial obstacle in the use of a fully atomistic model in order to make useful predictions. In recent years, a very promising method known as the quasicontinuum (QC) method has been developed to circumvent this length scale problem (Tadmor *et al.* 1996, Shenoy *et al.* 1999a, Knap and Ortiz, 2001, Miller and Tadmor 2003). By using kinematic constraints through finite element interpolation, the method allows for developing atomic-scale resolution near defects while exploiting coarser description further away in order to reduce redundant degrees of freedom. This allows for an accurate description of a system while using less computational resources than a fully atomistic model.

The QC method has received broad attention since its debut, due to its theoretical elegance in thinning redundant degrees of freedom as well as its computational generality in treating a wide range of problems relating to defect nucleation and evolution in solids. For example, the method has been used to study nanoindentation (Tadmor *et al.* 1999, Shenoy *et al.* 2000), fracture (Miller *et al.*, 1998a; Miller *et al.* 1998b), grain boundaries (Shenoy *et al.* 1998), dislocations (Rodney and Phillips 1999) and phase transformation (Tadmor *et al.* 2002). These examples all share a common feature that the collective behavior of defects occurs at an intermediate length scale, often beyond the reach of atomistic modeling. Conversely, this collective behavior is difficult to resolve accurately using a continuum description alone. The QC method was originally developed for solving static equilibrium problems but has recently been extended to treat coarse-grained finite temperature problems (Shenoy *et al.* 1999b, Kulkarni 2007).

In spite of its success, the formulation of QC conceived and developed by Tadmor *et al.* (1996) and Shenoy *et al.* (1999a) has an inherent inadequacy in the calculation of forces in the area of transition between the fully atomistic and continuum regions. Due to the mismatch between non-local atoms and local continuum, non-physical forces (a.k.a. ghost forces) arise even for an unstressed perfect crystal, *let alone* for more demanding inhomogeneous phenomena. Ghost forces can be partially corrected by adding dead loads to the energy functional. However, such treatment might lead to additional spurious effects if the initial deformation across the local and non-local interface is non-uniform (Curtin and Miller 2003). The non-uniformity can easily occur when the neighboring non-local atoms are perturbed from their periodical configurations.

These difficulties motivate us to develop a quasicontinuum method to transmit inhomogeneity from the atomistic to the continuum regions and to resolve the mathematical mismatch between non-local atoms and local continuum. In particular, we are interested in developing the correct energy and force formulation for the Cauchy-Born based QC method. To this end, errors due to an improper application of the Cauchy-Born rule at the non-local and local interface are analyzed. The analysis naturally leads to the need of a new class of transition entities if the QC method is to be applied.

In the next section of the paper, energy and force calculations solely under the kinematic constraint assumption are provided; these calculations serve as a desirable benchmark to be reproduced by their calculations using a reduced number of degrees of freedom. Energy and force calculations to cope with non-local and local transition elements in order to reproduce this benchmark are derived in Section 3. In addition, a cutoff sampling method is derived to identify and elucidate the root of non-locality in the transition region. The major roles of transition elements in the QC method are analyzed in detail in Section 4. Finally, numerical examples in two and three dimensional systems are given to demonstrate the accuracy and possible applications of the proposed method.

2. The kinematic constraint assumption

The basic machinery for the QC method is the concept of kinematic constraints through finite element interpolation. Consider a set of n atoms Ω with the Cartesian positions $\mathbf{r}_1, \mathbf{r}_2, \dots, \mathbf{r}_n$ in space (Fig. 1(a)). In the classical molecular dynamics (MD) or static molecular analysis, the total potential energy E_{MD} , in the absence of external potential, can be calculated through the summation of the energy of each individual atom so that

$$E_{MD} = \sum_{i \in \Omega} E_i(\mathbf{r}_1, \mathbf{r}_2, \dots, \mathbf{r}_n) \quad (1)$$

Here E_i is the energy of an atom i . The basic assumption for the QC method is to assert that some atoms are kinematically constrained by the others and dubbed “slaved” atoms herein. The position of a slaved atom \mathbf{r}_s can be represented by the positions of a set of representative atoms \mathbf{r}_α through a finite element shape function

$$\mathbf{r}_s = \sum_{\alpha \in L_s} N_\alpha(\mathbf{r}_s) \mathbf{r}_\alpha \quad (2)$$

where s and α denote the slaved and representative atoms, L_s denotes the set of representative atoms for the slaved atom s , and $N_\alpha(\mathbf{r}_s)$ are the shape function values at \mathbf{r}_s . For example, consider a slaved atom d in Fig. 1(b). In the QC method the slaved atom d can be represented by the representative atoms a, b, c where $L_d = \{a, b, c\}$.

Under the kinematic constraint assumption, the total energy of Ω for the QC method can be written as

$$E_{KC} = \sum_{i \in \Omega} E_i(\mathbf{r}_1, \mathbf{r}_2, \dots, \mathbf{r}_m, \mathbf{r}_{m+1}(L_{m+1}), \dots, \mathbf{r}_n(L_n)) = \sum_{i \in \Omega} E_i(\mathbf{r}_1, \mathbf{r}_2, \dots, \mathbf{r}_m) \quad (3)$$

Here $\mathbf{r}_1, \mathbf{r}_2, \dots, \mathbf{r}_m$ denote the positions of the representative atoms $m \leq n$. The force for a representative atom η can be obtained by taking the negative derivative of the total energy

$$\mathbf{f}_\eta^{KC} = -\frac{\partial E_{KC}}{\partial \mathbf{r}_\eta} = -\sum_{i \in \Omega} \frac{\partial E_{KC}}{\partial \mathbf{r}_i} \frac{\partial \mathbf{r}_i}{\partial \mathbf{r}_\eta} = \sum_{i \in \Omega} \left(\mathbf{f}_i^{MD} \frac{\partial \mathbf{r}_i}{\partial \mathbf{r}_\eta} \right).$$

Using Eq. (2), the force for a representative atom η then becomes

$$\mathbf{f}_\eta^{KC} = \sum_{i \in \Omega} \left(\mathbf{f}_i^{MD} N_\eta(\mathbf{r}_i) \right) \quad (4)$$

It is worth noting that the energy and force calculations in Eqs. (3) and (4) are a sum over the total n atoms, so further approximation is always needed to reduce the sum. Nevertheless, these are the solutions that result directly from kinematically constrained MD and serve as a desirable benchmark for different variants of QC formulations to be reproduced upon. The formulation by

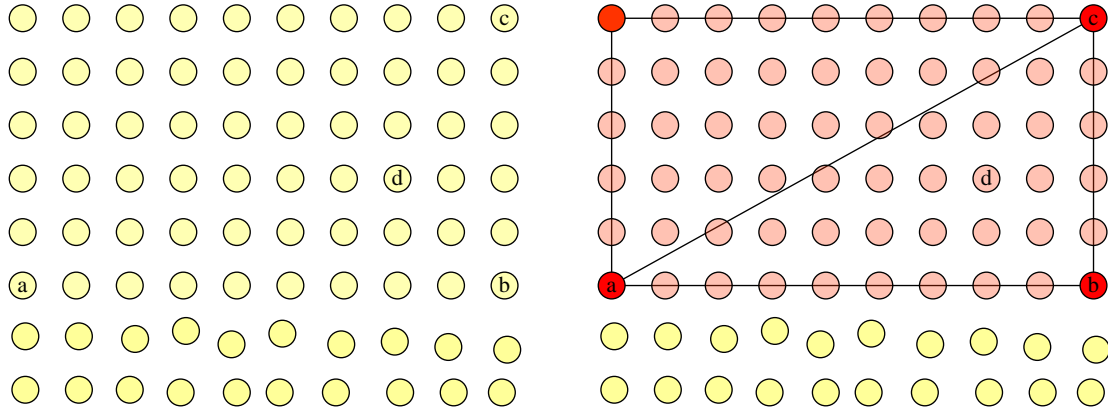


Fig. 1 (a) The n atom configuration in MD and (b) the m atom configuration in QC

Tadmor *et al.* (1996) and Shenoy *et al.* (1999a) used the Cauchy-Born rule to reduce the sum while Knap and Ortiz (2001) applied the cluster sampling and summation rules. In this work, we shall mainly focus on how to reproduce the energy and force calculations given in Eqs. (3) and (4) under the framework of the Cauchy-Born rule.

3. Energy and force calculations with transition elements

3.1 Energy calculations

Two related issues on energy calculations are discussed in this section. The first concerns the error resulting from an improper application of the Cauchy-Born rule at the local and non-local interface. The second deals with the correction of the error and the reproduction of Eq. (3) with transition elements.

Consider a typical set of representative and slaved atoms, as shown in Fig. 2, where deformation gradients are uniform in the local region and are non-uniform in the non-local region. Let Ω denote the set of total atoms and R denote the set of representative atoms. The set R can be further decomposed into two sets L and A , where L denotes the set of local representative atoms and A denotes non-local representative atoms. The set of slaved atoms is defined by the difference of Ω and R , such that $S = \Omega \setminus R$. Eq. (3) can thus be rewritten as

$$E_{KC} = \sum_{\beta \in A} E_{\beta}(\mathbf{r}_1, \mathbf{r}_2, \dots, \mathbf{r}_m) + \sum_{\alpha \in L} E_{\alpha}(\mathbf{r}_1, \mathbf{r}_2, \dots, \mathbf{r}_m) + \sum_{s \in S} E_s(\mathbf{r}_1, \mathbf{r}_2, \dots, \mathbf{r}_m) \quad (5)$$

Here the first term is the energy of non-local representative atoms which should be calculated using an atomistic method. The second and third terms are the energies of the local region contributed from the local representative atoms and slaved atoms, respectively. Under the framework of the Cauchy-Born rule, the energy of the slaved atoms in the QC method can be represented by the local representative atoms

$$\sum_{\alpha \in L} E_{\alpha} + \sum_{s \in S} E_s \approx \sum_{\alpha \in L} n_{\alpha} E_{\alpha} \quad (6)$$

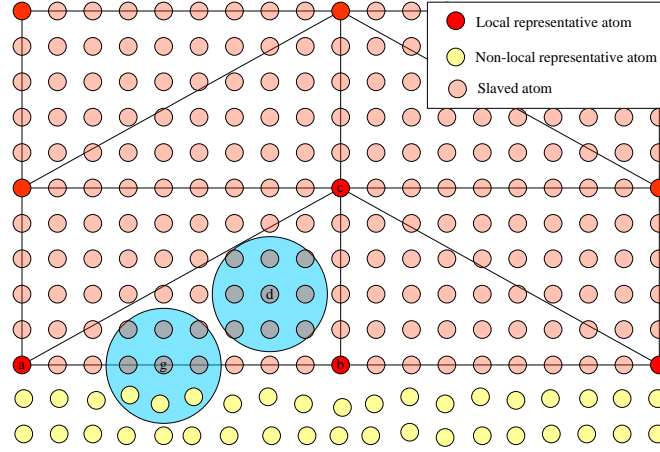


Fig. 2 Representative and slaved atoms at the transition region in the conventional QC method

where E_α is calculated by the Cauchy-Born rule and n_α is a weight function. Therefore, the total energy of the local region is only a sum over the elements. The energy of each element can be approximated to be $v_e \varepsilon(\mathbf{F}_e)$, where $\varepsilon(\mathbf{F}_e)$ is the strain energy density on the basis of the element deformation gradient \mathbf{F}_e and v_e is the volume of an element e (Shenoy *et al.*, 1999a). If M denotes the set of elements, Eq. (6) becomes

$$\sum_{\alpha \in L} n_\alpha E_\alpha = \sum_{e \in M} v_e \varepsilon(\mathbf{F}_e) \quad (7)$$

Therefore, the total energy in Eq. (5) is reduced to:

$$E_{KC} \approx E_{QC} = \sum_{e \in M} v_e \varepsilon(\mathbf{F}_e) + \sum_{\beta \in A} E_\beta \quad (8)$$

All the energies of slaved atoms are calculated by the Cauchy-Born rule in this approximation, regardless of whether a slaved atom is close to or far away from the non-local region. That is, energies of two atoms d and g shown in Fig. 2 have the same atomic energy, both calculated by the Cauchy-Born rule. It is thus evident that such approximation is not correct for the slaved atom g .

The energy for a slaved atom near the non-local region cannot be satisfactorily approximated by the Cauchy-Born rule and needs to be resolved using atomistic calculations. To this end, slaved atoms are decomposed into two sets: pure slaved atoms S^P whose energies can be computed by the Cauchy-Born rule and transition slaved atoms S^T whose energies need to be computed individually. That is

$$S^T = \{ S \mid S \in \text{and } J_s^A \neq J \emptyset \} \quad (9)$$

where J_s^A denotes for the subset of non-local representative atoms A within the cutoff of the

transition slaved atom s . The pure slaved atoms can then be defined by the difference of S and S^T , i.e. $S^P = S \setminus S^T$.

The separation of slaved atoms naturally leads to two types of local representative atoms. One is the transition representative atoms T that are either within the cutoff of non-local representative atoms or representing some transition slaved atoms such that

$$T = \left\{ \alpha \mid \alpha \in L_s \text{ and } J_\alpha^A \neq \emptyset \right\} \cup \left\{ \alpha \mid \exists s \text{ s.t. } \alpha \in L_s \text{ and } s \in S^T \right\} \quad (10)$$

The other is the pure local representative atoms L^P that are the difference of L and T , i.e. $L^P = L \setminus T$. All the representative and slaved atoms resulting from transition slaved atoms are illustrated in Fig. 3. Similarly, elements are now divided into three kinds. The first is the non-local transition elements M_{NL}^T which are close to the non-local and local interface; these elements contain some transition slaved atoms. The second is the local transition elements M_L^T which are adjacent to the non-local transition elements; these elements contain no transition slaved atoms while at least one of the element's nodes is a transition representative atom. The third is the pure local elements M^P found far away from the non-local region; these elements contain no transition slaved atoms and all of the element's nodes are pure local representative atoms.

In order to correct the error from an improper application of the Cauchy-Born rule at the local and non-local interface, the correct energy contribution from the transition slaved atoms need to be taken into account. The desirable reduced energy equations to reproduce Eq. (3) become

$$E_{KC} = E'_{QC} = \sum_{\beta \in A} E_\beta + \sum_{e \in M^P \cup M_L^T} v_e \mathcal{E}(\mathbf{F}_e) + \sum_{e \in M_{NL}^T} v'_e \mathcal{E}(\mathbf{F}_e) + \sum_{s \in S^T} E_s + \sum_{\alpha \in T^T} E_\alpha \quad (11)$$

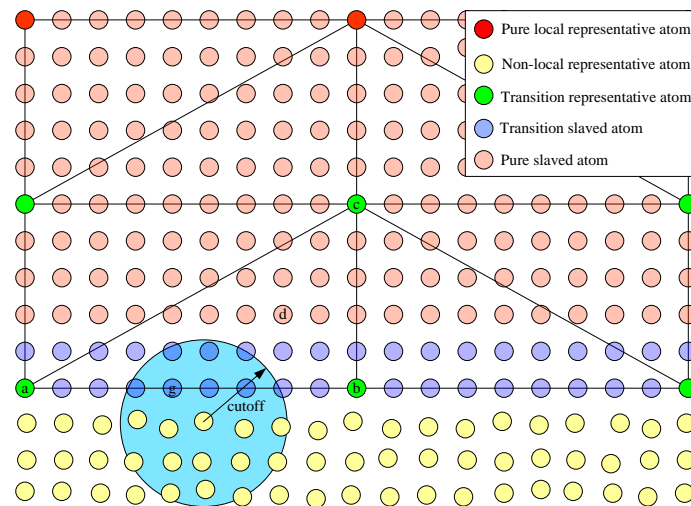


Fig. 3 Representative and slaved atoms resulting from transition slaved atoms

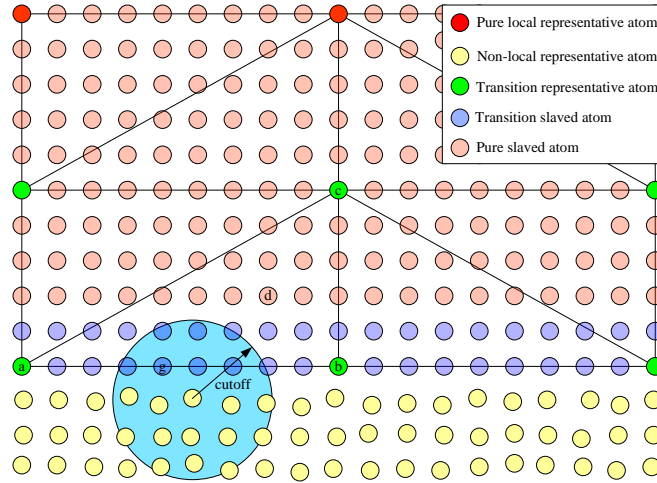


Fig. 4 Illustration of S_η for a transition representative atom η

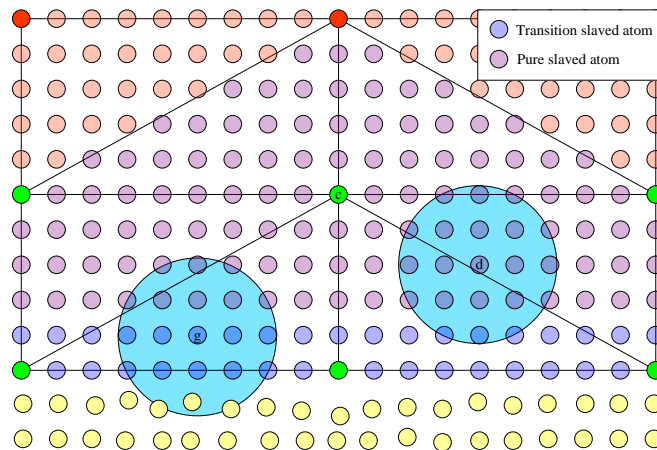


Fig. 5 Pure slaved atoms d and transition slaved atoms g and their neighboring atoms'

where T^T is a subset of transition representative atoms lying within the cutoff of the non-local representative atoms. The first two terms in Eq. (11) are the conventional energy contributions from the non-local and local regions respectively (Shenoy *et al.*, 1999a). The last three terms in Eq. (11) are the energies from the transition region. v'_e is a modified volume term which subtracts out the volumetric contributions from the transition slaved atoms and transition representative atoms in an element e . The energies of transition slaved and transition representative atoms need to be resolved through atomistic calculations, looping through their neighboring atoms within the potential cutoff.

3.2 Force calculations

In this section, we discuss the force calculations of the representative atoms under the framework of Cauchy-Born rule with an aim to reproduce Eq. (4). To this end, we compare the

negative derivatives of E'_{QC} from Eq. (11) with the forces evaluated from Eq. (4). As a result the derivatives reproduce the forces for the non-local and local representative atoms in Eq. (4). However this does not hold for the transition representative atoms; a new set of force calculations directly reduced from Eq. (4) for transition representative atoms must be derived.

We start investigating the issues related to force calculations by taking the negative derivatives of Eq. (11)

$$-\frac{\partial E'_{QC}}{\partial \mathbf{r}_\eta} = -\left(\sum_{\beta \in A} \frac{\partial E_\beta}{\partial \mathbf{r}_\eta} + \sum_{e \in M^P \cup M^T_L} v_e \frac{\partial \mathcal{E}(\mathbf{F}_e)}{\partial \mathbf{r}_\eta} + \sum_{e \in M^T_{NL}} v'_e \frac{\partial \mathcal{E}(\mathbf{F}_e)}{\partial \mathbf{r}_\eta} + \sum_{s \in S^T} \frac{\partial E_s}{\partial \mathbf{r}_\eta} + \sum_{\alpha \in T^T} \frac{\partial E_\alpha}{\partial \mathbf{r}_\eta} \right) \quad (12)$$

To evaluate whether Eq. (12) reproduces Eq. (4), we compare these two equations for non-local, local, and transition representative atoms, respectively. First, for a non-local representative atom β , the second and third terms vanish since they are not a function of non-local atoms. The remaining three terms are all calculated atomistically, thus only those atoms lying within β 's cutoff remain in effect, so that

$$\mathbf{f}_\beta^{QC} = -\frac{\partial E'_{QC}}{\partial \mathbf{r}_\beta} = -\frac{\partial E_\beta}{\partial \mathbf{r}_\beta} + \sum_{j \in J_\beta} -\frac{\partial E_j}{\partial \mathbf{r}_\beta} = \mathbf{f}_\beta^{MD} \quad (13)$$

where J_β denotes the set of atoms within the cutoff of the atom β . Let us now consider the force calculations from Eq. (4) for a non-local representative atom β

$$\mathbf{f}_\beta^{KC} = \sum_{i \in \Omega} (\mathbf{f}_i^{MD} N_\beta(\mathbf{r}_i)) = \mathbf{f}_\beta^{MD}$$

where we have used the fact that for a non-local representative atom β , $N_\beta(\mathbf{r}_i) = \delta_{\beta i}$. Thus it is evident that the derivatives of E'_{QC} have reproduced the forces in Eq. (4) for the non-local representative atoms.

Second, we consider the case for a pure local representative atom $\alpha \in L^P$. Since, by definition, the pure local representative atom is far away from the transition region, it is obvious that only the second term in Eq. (12) remains in effect. The derivatives thus reduce to the well-known Cauchy-Born forces (Shenoy *et al.* 1999a)

$$\mathbf{f}_\alpha^{QC} = -\frac{\partial E'_{QC}}{\partial \mathbf{r}_\alpha} = -\sum_{e \in M_\alpha} v_e \mathbf{P}(\mathbf{F}_e) \nabla_0 N_\alpha(\mathbf{r}_e) \quad (14)$$

where M_α denotes α 's adjacent elements, $\mathbf{P}(\mathbf{F}_e)$ is the first Piola-Kirchhoff stress and ∇_0 is the gradient with respect to a reference configuration. Since α is a pure local representative atom, the neighboring atomic configuration is, by definition, homogeneous. It is therefore, straightforward to show that Eq. (14) reproduces Eq. (4).

Finally, for a transition representative atom, the derivatives of E'_{QC} given in Eq. (12) are not sufficient to reproduce the results in Eq. (4). This is due to two facts: mathematical mismatch and

physical non-locality. The mathematical mismatch occurs due to the well-known incompatibility between local continuum and non-local atoms (Curtin and Miller 2003). The issue associated with physical non-locality is caused by the breakdown of the Cauchy-Born rule in a similar way to that in the energy calculations. In short, the forces for the transition slaved atoms cannot be satisfactorily computed by the Cauchy-Born rule; they must be resolved atomistically. We shall revisit these two facts in Section 4 and discuss the roles played by the non-local transition elements, local transition elements and transition representative atoms in resolving the issues.

To this end, we use Eq. (4) directly to evaluate the forces for transition representative atoms. To simplify Eq. (4) for a transition representative atom η , the delta function is introduced

$$\mathbf{f}_\eta^{KC} = \sum_{\beta \in A} \delta_{\beta\eta} \mathbf{f}_\beta^{MD} + \sum_{\alpha \in L} \delta_{\alpha\eta} \mathbf{f}_\alpha^{MD} + \sum_{s \in S} \mathbf{f}_s^{MD} N_\eta(\mathbf{r}_s)$$

For the transition representative atom, the first summation vanishes and only one term in the second summation remains in effect. The force calculations for a transition representative atom η thus become

$$\mathbf{f}_\eta^{QC} = \mathbf{f}_\eta^{MD} + \sum_{s \in S_\eta} \mathbf{f}_s^{MD} N_\eta(\mathbf{r}_s) \quad (15)$$

where S_η is the set of slaved atoms that have η as one of their representative atoms (Fig. 4).

Two further remarks are given. First, the force of a transition representative atom is obtained from summing the atomic forces of the corresponding slaved atoms weighted by their shape function values. Second, although calculating force on a transition representative atom η requires looping through all the slaved atoms represented by it, such computation is relatively inexpensive due to the fact that the number of transition representative atoms is far less than those of non-local and local representative atoms.

We now proceed to show that a synthesis exists for the energy and force calculations in the transition region. That is, all the non-locality is induced from the neighboring non-local representative atoms near the transition region. Let us decompose S_η into two subsets: pure slaved atoms S_η^P and transition slaved atoms S_η^T (Fig. 5). Eq. (15) thus becomes

$$\mathbf{f}_\eta^{QC} = \mathbf{f}_\eta + \sum_{s \in S_\eta^T} \mathbf{f}_s^{MD} N_\eta(\mathbf{r}_s) + \sum_{s \in S_\eta^P} \mathbf{f}_s^{MD} N_\eta(\mathbf{r}_s) \quad (16)$$

In the last term of Eq. (16), the summation is carried over all the pure slaved atoms. By definition, the pure slaved atoms should have the same periodical environment under the Cauchy-Born rule. For example, pure slaved atoms g and h in Fig. 5 have the same neighboring environment, i.e., $f_g = f_h$. Thus, Eq. (16) reduces to

$$\mathbf{f}_\eta^{QC} = \mathbf{f}_\eta + \sum_{s \in S_\eta^T} \mathbf{f}_s^{MD} N_\eta(\mathbf{r}_s) + \mathbf{f}_\xi^{MD} \sum_{s \in S_\eta^P} N_\eta(\mathbf{r}_s), \quad (17)$$

where ξ is an arbitrary atom in S_η^P . Eq. (17) offers very important implications for developing an effective scheme to compute forces using the QC method in general. For the case of radially

symmetric potentials in the homogeneous region, we simply have $\mathbf{f}_\xi = \mathbf{0}$. Thus the last term vanishes and Eq. (16) reduces to

$$\mathbf{f}_\eta^{QC} = \mathbf{f}_\eta + \sum_{s \in S_\eta^T} \mathbf{f}_s^{MD} N_\eta(\mathbf{r}_s) \quad (18)$$

Since the sampling atoms only lie within a potential cutoff distance from non-local representative atoms, the force formulation given in Eq. (18) is referred to as the ‘‘cutoff sampling method’’ herein. Meanwhile, the formulation given in Eq. (15) is referred to as the ‘‘fully sampling method.’’ The force formulation in Eq. (18) offers a clear physical insight; all the non-locality originates from the fact that the transition representative atoms and transition slaved atoms both require atomistic treatment since they are within the cutoff of non-local representative atoms. By taking such non-locality into account, we can satisfactorily reproduce the energy and force evaluated from kinematically constrained MD under the framework of the Cauchy-Born rule.

4. Analysis of transition elements

An illustrative analysis of the two roles of transition elements in QC analysis is given in this section. The first is to resolve the mathematical mismatch between the regions that are calculated atomistically and as a continuum using local transition elements while the second is to transit inhomogeneity from atomistic to continuum using non-local transition elements. Two distinct atomic configurations are used herein to demonstrate the roles. One configuration is an unstressed perfect crystal as shown in Fig. 6(a) with underlining atoms being arranged periodically in their equilibrium positions. Thus, the net force on each atom is zero. The other configuration contains an irregular arrangement of non-local representative atoms shown in Fig. 6(c); such irregular configuration is often encountered in QC practice.

First, an analysis of how the mathematical mismatch between the atomistic and continuum region is resolved by using force formulations is derived. The force of transition representative atom ‘‘a’’ shown in Fig. 6(a), is computed using Eq. (15) or (18). That is, the force of the transition representative atom ‘‘a’’ is obtained from the summation and weighting of the atomic forces of the slaved atoms highlighted in Fig. 6(b). For the pure local representative atom ‘‘b,’’ Eq. (14) is employed; all its adjacent elements are approximated as continuum elements. It is then obvious that local transition elements 1-4 in Fig. 6(a) and Fig. 6(b) have dual features. For transition representative atoms, the local transition elements serve as a convenient ‘‘holder’’ that contains a group of kinematically constrained atoms. For pure local representative atoms, the local transition elements possess Cauchy-Born behavior. As a result of these two features, the transition representative atom ‘‘a’’ can ‘‘see’’ the slaved atoms of the local transition elements while the pure local representative atoms cannot. Such treatments resolve the mathematical mismatch between atomistic and continuum, i.e. no ghost forces exist. Conceptually, the mismatch treatments given herein are similar to the ghost force correction method developed and discussed by Tadmor *et al.* (1996), Shenoy *et al.* (1999a) and Curtin and Miller (2003).

In addition to local transition element which resolves the mathematical mismatch between the atomistic and continuum regions, non-local transition elements serve as a bridge to transmit inhomogeneity from the former region to the latter. In Fig. 6(c), transition slaved atoms such as the

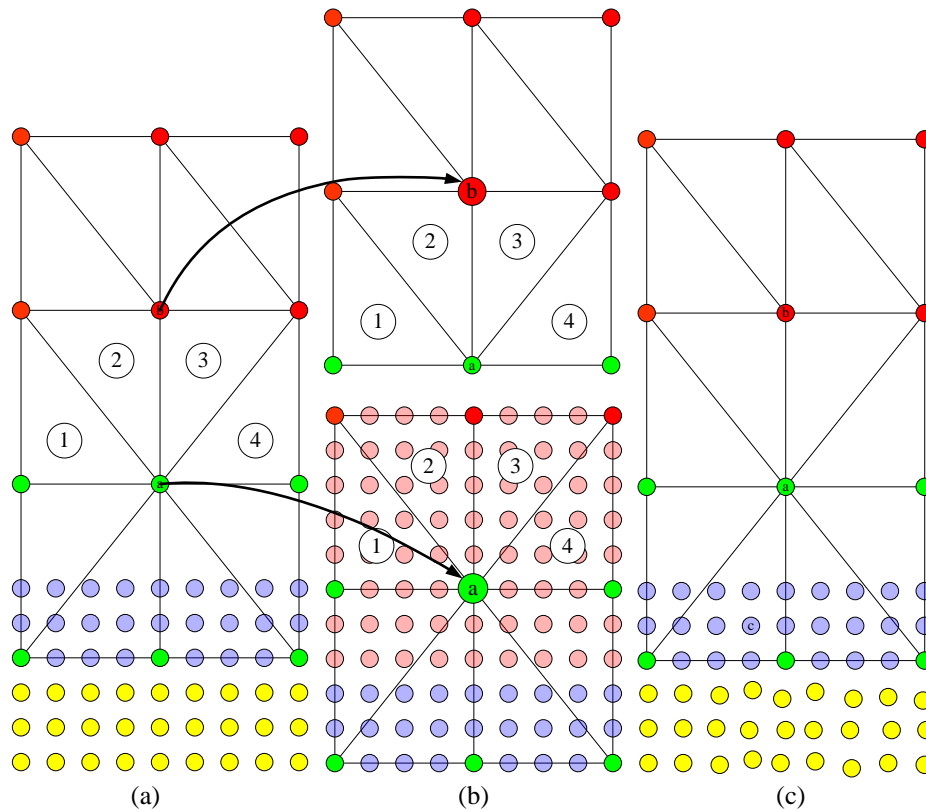


Fig. 6 Atomic and element configurations in (a) an unstressed perfect crystal with transition elements, (b) slaved atoms and elements for force calculations of transition representative atoms and pure local representative atoms, and (c) an inhomogeneous arrangement at the non-local region. Yellow atoms represent non-local representative atoms, green atoms represent transition representative atoms, red atoms represent pure local representative atoms, light blue atoms represent transition slaved atoms and light red atoms represent pure slaved atoms

atom “c” are treated atomistically. Such treatment is associated with the physical argument given in the aforementioned section; the forces on the transition slaved atoms cannot be satisfactorily computed by the Cauchy-Born rule as they must be resolved atomistically. The force of the transition representative atom “a” in Fig. 6(c) is again obtained from the summation and weighting of the atomic forces of the slaved atoms, but now contains the proper inhomogeneity induced by the non-local representative atoms.

5. Results and discussion

Three examples are used to demonstrate the accuracy and applicability of the proposed method. In the first two examples, we aim to verify the accuracy of the force formulation presented in the previous sections for various interatomic potentials and atomic configurations. The salient features of the transition entities are emphasized. In the last example, a 3D nanoindentation simulation is

conducted based on the adaptive procedure proposed in Shenoy *et al.* (1999a). Simulation results are compared with static equilibrium results from MD to validate the proposed method.

5.1 Force analysis using a Lennard-jones potential in 2D

We first use a 2D example to show that the ghost force problem is satisfactorily solved with the transition elements. To this end, three different QC models with a square lattice as shown in Fig. 7 are considered. Fig. 7(a) shows a conventional QC model with only local and non-local representative atoms. Fig. 7(b) and Fig. 7(c) show the QC models with transition elements. Force formulations given in Eq. (15) (the fully sampling method) and Eq. (18) (the cutoff sampling method) were adopted for the QC models in Fig. 7(b) and Fig. 7(c), respectively.

For simplicity, the 6-12 Lennard-Jones potential $\phi(r)$ was used

$$\phi(r) = 4\varepsilon \left[\left(\frac{\sigma}{r} \right)^{12} - \left(\frac{\sigma}{r} \right)^6 \right],$$

where σ and ε are adjustable parameters to characterize the length and energy scales, respectively. A 2.5σ potential cutoff was used. The forces on the representative atoms were calculated based on these configurations. As all underlining atoms have been arranged in their equilibrium positions, the total force on each atom should be zero for the unstressed perfect crystal.

Computed forces resulting from these models are plotted in Fig. 8. The results confirm the existence of non-zero ghost forces in the conventional QC model where the transition formulation is not considered. As expected, the ghost force problem is satisfactorily solved for the QC models when transition elements are employed. Furthermore, the cutoff sampling method yields identical results to the fully sampling method.

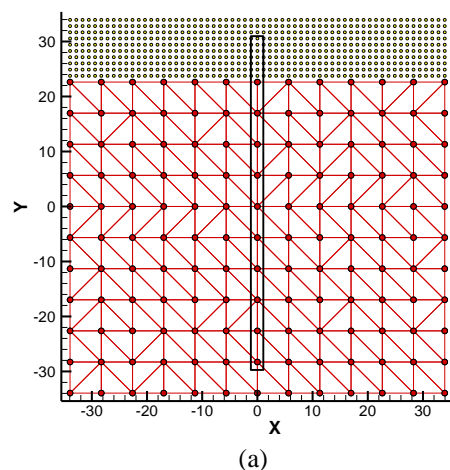
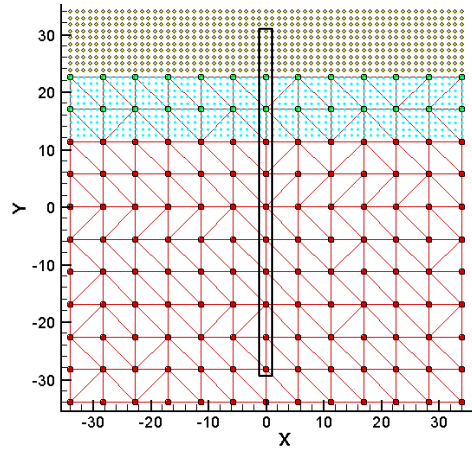
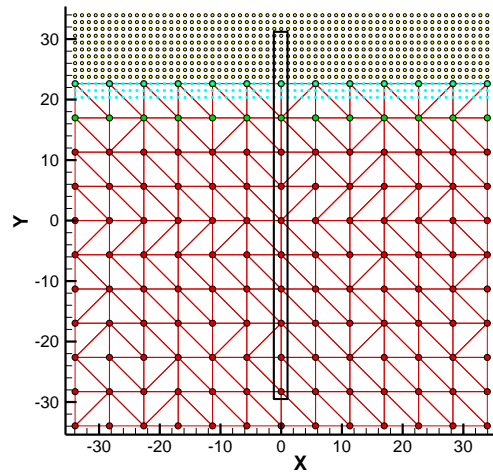


Fig. 7 Square lattice QC models using a (a) convention layout, (b) layout for fully sampling method, and (c) layout for cutoff sampling method. The light blue atoms correspond to the transition slaved atoms used in these methods



(b)



(c)

Fig. 7 Continued

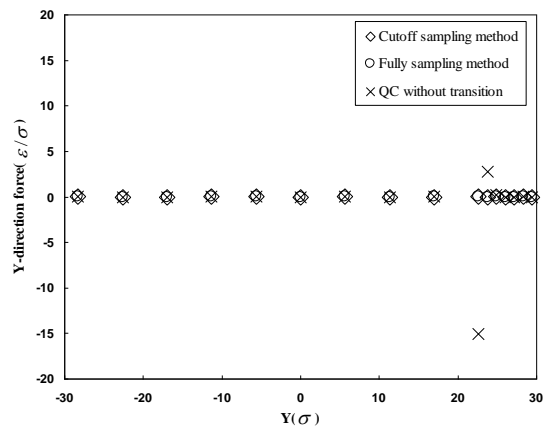


Fig. 8 Y-direction force for different QC models in an unstressed perfect crystal

5.2 Force analysis for a grain boundary in 3D using an EAM potential

We next consider a simple tilt grain boundary in 3D to demonstrate the inhomogeneity induced from non-local representative atoms. In addition, forces of the transition slaved atoms and transition representative atoms need to be resolved atomistically within these non-local representative atoms' cutoff.

A tilt grain boundary model of face-centered cubic (FCC) aluminum is shown in Fig. 9. The model was constructed by rotating the right part of the grain by 45 degrees around the Y axis. The lattice spacing is 4.032 \AA . A cross section of the $\{001\}$ plane is shown in Fig. 9(b).

Aluminum was modeled using the embedded-atom potential developed by Ercolessi and Adams (1994). Fig. 10 plots the forces of representative atoms in the X-direction marked in Fig. 9(b). It shows again that those forces obtained from the fully sampling method (Eq. (15)) and the cutoff sampling method (Eq. (18)) yield identical results.

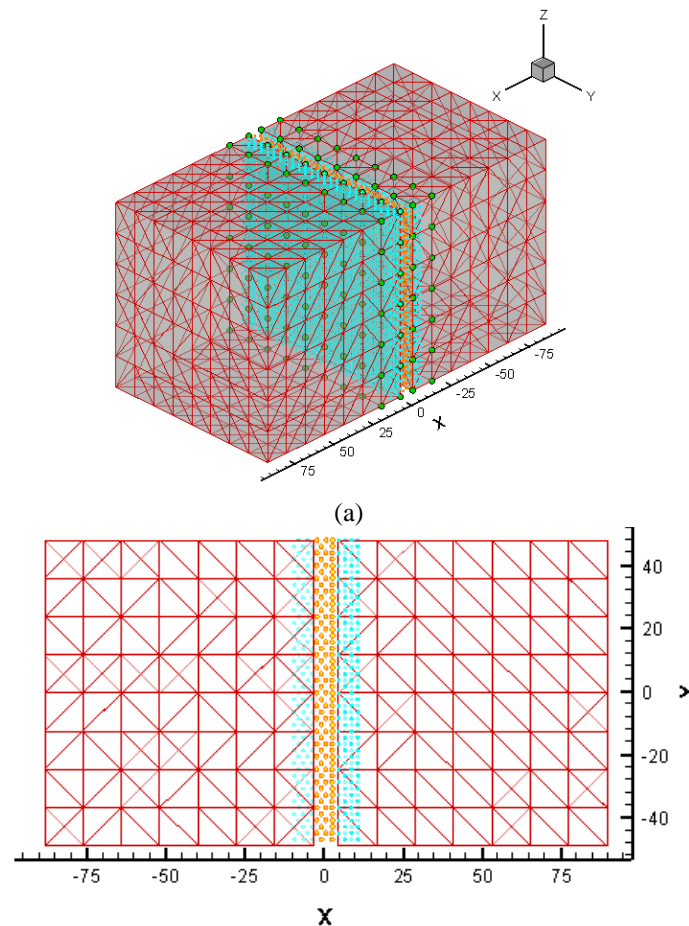


Fig. 9. (a) Layout of an unrelaxed grain boundary model and (b) atomic configurations from top view of the model. Orange and light blue atoms correspond to the non-local representative atoms and transition slaved atoms, respectively

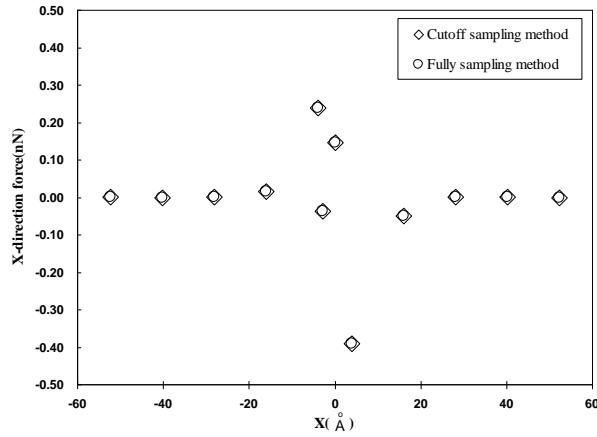


Fig. 10 X-directional forces across the unrelaxed grain boundary

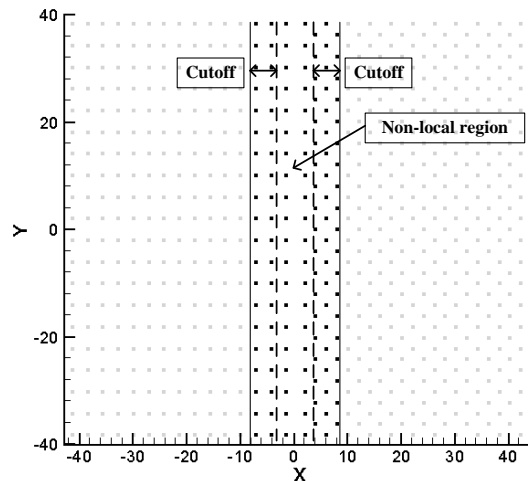


Fig. 11 Highlights of non-zero force field (indicated by black dots) from a fully atomistic model

Finally, non-localities that occur at the transition region in the QC method are studied. To this end, a fully atomistic model was constructed and the atomic forces were calculated using MD. Fig. 11 highlights the non-zero forces for the atoms on the $z=0$ plane. In the QC model we observe that non-zero atomic forces occur at the non-local region and at the transition region within a cutoff distance of non-local atoms. It is evident that the Cauchy-Born rule is no longer valid for these atoms. Thus, we conclude that transition treatments formalized in this study are needed in order to take these inhomogeneities into account.

5.3 Nanoindentation simulation in 3D

Nanoindentation simulations in 3D using the MD and QC methods were carried out in parallel to illustrate the accuracy of the transition formulation proposed herein. A thin film FCC aluminum

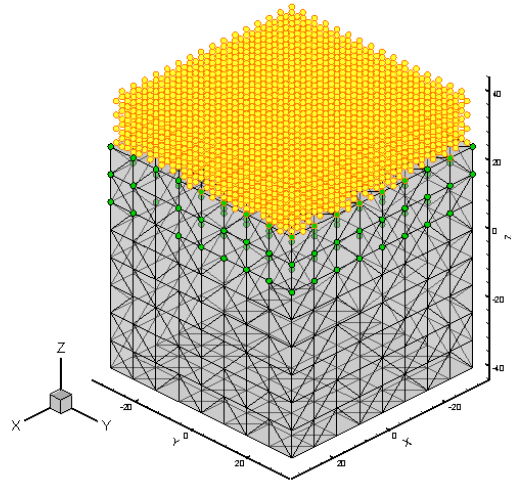


Fig. 12 QC initial model: the yellow atoms are non-local representative atoms and the green atoms are transition representative atoms

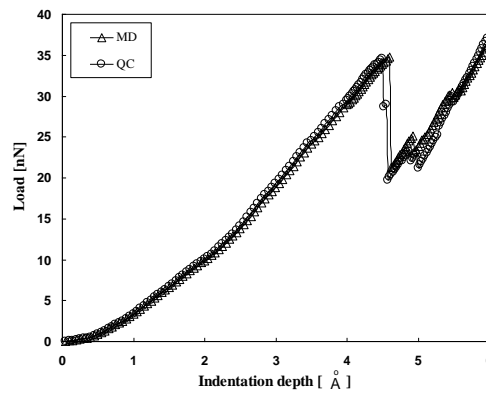


Fig. 13 Load-displacement curves for nanoindentation simulation

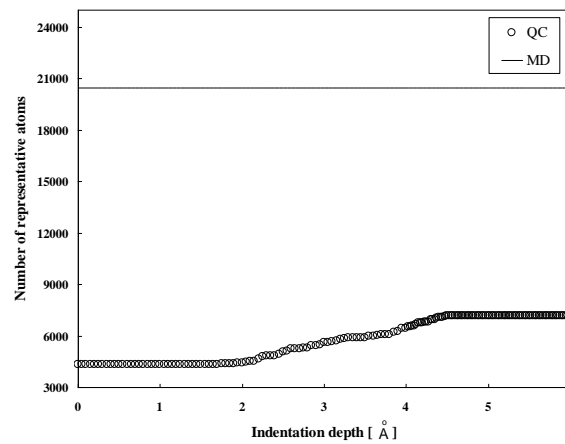


Fig. 14 Number of evolving representative atoms in the QC model

sample was modeled by a $50 \text{ \AA} \times 50 \text{ \AA} \times 80 \text{ \AA}$ box. Periodic boundary conditions along the X and Y directions were applied in the MD model and in the non-local and transition regions in the QC model. Fixed boundary conditions at the bottom were applied in both models. The number of atoms in the MD model was 20,480. The initial QC model is shown in Fig. 12(a) in which a block of fully-refined non-local representative atoms were constructed in the vicinity of the indentation region to capture surface effects. The total number of representative atoms in the initial QC model was 4,313.

Nanoindentation simulations were carried out by driving a spherical indenter into the simulated sample along the Z direction. The embedded-atom potential developed by Ercolessi and Adams (1994) was used to model the aluminum thin film. In addition, the force relationship between the atoms of the aluminum sample and the indenter was described by an indenter-sample interaction potential given by

$$f(r) = A(R - r)^2 \quad (19)$$

where R is the radius of the spherical indenter, r is the distance from the center of the indenter to an atom in the sample and A is a force coefficient. This example used a radius R of 12.5 \AA and a coefficient A of 10.

The simulation was performed by moving the indenter downward incrementally into the top surface of the samples. At each incremental step, an equilibrium configuration was obtained by using the Polak-Ribiere variation of the conjugate gradient method (Press *et al.*, 2000). For the QC method, the adaptive remeshing scheme used by Shenoy *et al.* (1999a) was adopted. The variation of the deformation gradient was used as the adaptation indicator with a preset tolerance of 0.005. At each incremental step, the mesh in the QC model was continuously adapted until the tolerance was met.

The computed load-displacement curves from the MD and QC methods are plotted in Fig. 13. An essentially elastic response is observed until dislocation nucleates at the first critical load. The MD model predicts the critical load of 34.81 nN at indentation depth of 4.6 \AA and the QC model predicts 34.58 nN at 4.5 \AA . The difference between the two models is about 0.66% and we can conclude that, overall, the QC results agree very well with those from MD. Figure 14 plots the evolution of the total number of representative atoms used in QC. The initial QC model is capable of capturing induced deformation until the indentation depth exceeds 2 \AA . Further mesh adaptation is observed until the first critical load is reached. The total number of representative atoms in the final refined QC model is 7,186.

6. Conclusions

We have formalized a QC method with non-local and local transition elements. New forms of energy and force calculations are derived by considering non-locality in a non-local transition element induced within the cutoff of non-local representative atoms and by considering reproduction of fully atomistic formulation imposed with kinematic constraints. The proposed energy formulation properly corrects the error from applying the Cauchy-Born rule at the local and non-local interface. Through summing and weighting the atomic forces of the transition slaved

atoms into the transition representative atoms, the new description of the force formulation allows non-local transition elements to correctly transmit inhomogeneity from the atomistic to the continuum regions. In addition, dual features of local transition elements possessed by the proposed force formulation allow one to eliminate undesirable ghost forces caused by the inherent mathematical mismatch between non-local atoms and the local continuum. We conclude that energy and force calculations with transition entities are indispensable for the Cauchy-Born based QC method developed by Tadmor *et al.* (1996) and Shenoy *et al.* (1999a).

Acknowledgements

Computational resources were provided by the National Center for High-Performance Computing and National Taiwan University. This research was supported by funding from the National Science Council of Taiwan (NSC 100-2628-E-002-035-MY3, NSC 100-2628-E-002-004, NSC 100-2627-E-002-001) and National Taiwan University (10R80920-05).

References

- Chan, C.Y., Chen, Y.Y., Chang, S.W. and Chen, C.S. (2011), "Atomistic studies of nanohardness size effects", *Int. J. Theoretical Appl. Multiscale Mech.*, **2**(1), 62-71.
- Chen, C.S., Wang, C.K. and Chang, S.W. (2008), "Atomistic simulation and investigation of nanoindentation, contact pressure and nanohardness", *Interact. Multiscale Mech.*, **1**(4), 411-422.
- Chen, J. and Lee, J.D. (2010), "Atomistic analysis of nano/micro biosensors", *Interact. Multiscale Mech.*, **3**(2), 111-121.
- Curtin, W.A., Miller, R.E. (2003), Atomistic/continuum coupling in computational materials science. *Modeling and Simulation in Materials Sciences and Engineering*, **11**, R33-R68.
- Jeong, J., Cho, M. and Choi, J. (2011), "Effective mechanical properties of micro/nano-scale porous materials considering surface effects", *Interact. Multiscale Mech.*, **4**(2), 107-122.
- Knap, J. and Ortiz, M. (2001), "An analysis of the quasicontinuum method", *J. Mech. Physics Solids*, **49**, 1899-1923.
- Kulkarni, Y. (2007), "Coarse-graining of atomistic description at finite temperature", Ph.D. Thesis, California Institute of Technology.
- Lai, C.W. and Chen, C.S. (2013), "Influence of indenter shape on nanoindentation: an atomistic study", *Interact. Multiscale Mech.*, **6**(3), 301-316.
- Miller, R., Ortiz, M., Phillips, R., Shenoy, V. and Tadmor, E.B. (1998a), "Quasicontinuum models of fracture and plasticity", *Eng. Fract. Mech.*, **61**, 427-444.
- Miller, R., Tadmor, E.B., Phillips, R. and Ortiz, M. (1998b), "Quasicontinuum simulation of fracture at the atomic scale", *Model. Simul. Mater. Sci. Eng.*, **6**, 607-638.
- Miller, R. and Tadmor, E.B. (2003), "The quasicontinuum method: overview, applications and current directions", *J. Comput.-Aided Mater. Des.*, **9**, 203-39.
- Press, W.H., Vetterling, W.T., Teukolsky, S.A. and Flannery, B.P. (2000), *Numerical Recipes in C++: The Art of Scientific Computing*, Second Edition, Cambridge University Press.
- Rodney, D. and Phillips, R. (1999), "Structure and strength of dislocation junctions: an atomic level analysis", *Phys. Rev. Lett.*, **82**, 1704-1707.
- Shen, L. (2013), "Molecular dynamics study of Al solute-dislocation interactions in Mg alloys", *Interact. Multiscale Mech.*, **6**(2), 127-136.
- Shenoy, V.B., Miller, R., Tadmor, E.B., Phillips, R. and Ortiz, M. (1998), "Quasicontinuum models of

- interfacial structure and deformation”, *Phys. Rev. Lett.*, **80**, 742-745.
- Shenoy, V.B., Miller, R., Tadmor, E.B., Rodney, D., Phillips, R. and Ortiz, M. (1999a), “An adaptive finite element approach to atomic scale mechanics - the quasicontinuum method”, *J. Mech. Physics Solids*, **47**, 611-641.
- Shenoy, V., Shenoy, V. and Phillips, R. (1999), “Finite temperature quasicontinuum methods”, *Mater. Res. Soc. Symp. Proc.*, 538, 465-471.
- Shenoy, V.B., Phillips, R. and Tadmor, E.B. (2000), “Nucleation of dislocations beneath a plane strain indenter”, *J. Mech. Phys. Solids*, **48**, 649-673.
- Tadmor, E.B., Ortiz, M. and Phillips, R. (1996), “Quasicontinuum analysis of defects in solids”, *Philosophical Magazine A*, **73**, 1529-1563.
- Tadmor, E.B., Miller, R. and Phillips, R. (1999), “Nanoindentation and incipient plasticity”, *J. Mater. Res.*, **14**, 2233-2250.
- Tadmor, E.B., Waghmare, U.V., Smith, G.S. and Kaxiras, E. (2002), “Polarization switching in PbTiO₃: An *ab initio* finite element simulation”, *Acta Mat.*, **50**, 2989-3002.
- Teng, H., Lee, C.H. and Chen, J.S. (2011), “On the continuum formulation for modeling DNA loop formation”, *Interact. Multiscale Mech.*, **4**(3), 219-237.
- Wang, Y.C., Wu, C.Y., Chen, C. and Yang, D.S. (2013), “Molecular dynamics studies of interaction between hydrogen and carbon nano-carriers”, *Interact. Multiscale Mech.*, **6**(3), 271-286.
- Zhao, H. and Aluru, N.R. (2008), “Molecular dynamics simulation of bulk silicon under strain”, *Interact. Multiscale Mech.*, **1**(2), 303-315.